RESEARCH ARTICLE

WILEY Genetic Epidemiology

Multi-SKAT: General framework to test for rare-variant association with multiple phenotypes

Diptavo Dutta[1,2] | Laura Scott[1,2] | Michael Boehnke[1,2] | Seunggeun Lee[1,2]

[1]Department of Biostatistics, University of Michigan, Ann Arbor, Michigan

[2]Center for Statistical Genetics, University of Michigan, Ann Arbor, Michigan

Correspondence
Seunggeun Lee, Department of Biostatistics, University of Michigan, 1420 Washington Heights, Ann Arbor, MI 48105.
Email: leeshawn@umich.edu

Abstract

In genetic association analysis, a joint test of multiple distinct phenotypes can increase power to identify sets of trait-associated variants within genes or regions of interest. Existing multiphenotype tests for rare variants make specific assumptions about the patterns of association with underlying causal variants, and the violation of these assumptions can reduce power to detect association. Here, we develop a general framework for testing pleiotropic effects of rare variants on multiple continuous phenotypes using multivariate kernel regression (Multi-SKAT). Multi-SKAT models affect sizes of variants on the phenotypes through a kernel matrix and perform a variance component test of association. We show that many existing tests are equivalent to specific choices of kernel matrices with the Multi-SKAT framework. To increase power of detecting association across tests with different kernel matrices, we developed a fast and accurate approximation of the significance of the minimum observed P value across tests. To account for related individuals, our framework uses random effects for the kinship matrix. Using simulated data and amino acid and exome-array data from the METabolic Syndrome In Men (METSIM) study, we show that Multi-SKAT can improve power over single-phenotype SKAT-O test and existing multiple-phenotype tests, while maintaining Type I error rate.

KEYWORDS
Copula, gene-based test, METSIM study, multiple phenotypes, phenotype kernel, pleiotropy, rare variants, related individuals, SKAT

1 | INTRODUCTION

Since the advent of array genotyping technologies, genome-wide association studies (GWASs) have identified numerous genetic variants associated with complex traits. Despite these many discoveries, GWAS loci explain only a modest proportion of heritability for most traits. This may be due, in part, to the fact that these association studies are underpowered to identify associations with rare variants (Korte & Farlow, 2013). To identify such rare-variant associations, gene- or region-based multiple variant tests have been developed (Lee, Abecasis, Boehnke, & Lin, 2014). By jointly testing rare variants in a target gene or region, these methods can increase power over a single-variant test and are now used as a standard approach in rare-variant analysis.

Recent GWAS results have shown that many GWAS loci are associated with multiple traits (Solovieff, Cotsapas, Lee, Purcell, & Smoller, 2013). Nearly, 17% of variants in National Heart Lung and Blood Institute (NHLBI) GWAS categories is associated with multiple traits (Sivakumaran et al., 2011). For example, 44% of

autoimmune risk single-nucleotide polymorphisms (SNPs) has been estimated to be associated with two or more autoimmune diseases (Cotsapas et al., 2011). Detecting such pleiotropic effects is important to understand the underlying biological structure of complex traits. In addition, by leveraging cross-phenotype associations, the power to detect trait-associated variants can be increased.

Identifying the cross-phenotype effects requires a suitable joint or multivariate analysis framework that can leverage the dependence of the phenotypes. Various methods have been proposed for multiple-phenotype analyses in GWAS (Ferreira & Purcell, 2009; Huang, Johnson, & O'Donnell, 2011; Ray, Pankow, & Basu, 2016; Ried et al., 2012; Zhou & Stephens, 2014). Extending them, several groups have developed multiple-phenotype tests for rare variants (Broadaway et al., 2016; Lee et al., 2016; Maity, Sullivan, & Tzeng, 2012; Sun et al., 2016; Wang et al., 2015; Wu & Pankow, 2016; Yan et al., 2015; Zhan et al., 2017). For example, Wang et al. (2015) proposed a multivariate functional linear model (MFLM); Broadaway et al. (2016) used a dual-kernel-based distance-covariance approach to test for cross-phenotype effects of rare variants by comparing similarity in multivariate phenotypes to similarity in genetic variants (GAMuT; Chiu et al., 2017); Wu and Pankow (2016) developed a score-based sequence kernel association test for multiple traits, MSKAT, which has been shown to be similar in performance to GAMuT (Broadaway et al., 2016); Zhan et al. (2017) proposed a dual kernel based association test (DKAT), which uses the dual-kernel approach as in GAMuT but provides more robust performance when the dimension of phenotypes is high compared with the sample size.

Despite these developments, existing methods have important limitations. Most methods were developed under specific assumptions regarding the effects of the variants on multiple phenotypes, and hence lose power if the assumptions are violated (Ray et al., 2016). For example, if genetic effects are heterogeneous across multiple phenotypes, methods assuming homogeneous genetic effects can lose a substantial amount of power. Although there has been a recent attempt to combine analysis results from different models (Zhan et al., 2017), no scalable methods have been developed to evaluate the significance of the combined results in genome-wide scale analysis. In addition, most existing methods and software cannot adjust for relatedness between individuals; thus, to apply these methods, related individuals must be removed from the analysis to maintain Type I error rate. For example, in the METabolic Syndrome In Men (METSIM) study, ~15% of individuals is estimated to be related up to the second degree.

Here, we develop Multi-SKAT, a general framework that extends the mixed effect model-based kernel association tests to a multivariate regression framework while accounting for family relatedness. Mixed effect models have been widely used for rare-variant association tests. Popular rare-variant tests, such as SKAT (Wu et al., 2011) and SKAT-O (Lee, Wu, & Lin, 2012), are based on mixed effect models. By using kernels to relate genetic variants to multiple continuous phenotypes, Multi-SKAT allows for flexible modeling of the genetic effects on the phenotypes. The idea of using kernels for genotypes and phenotypes was previously used by the dual-kernel approaches, such as GAMuT and DKAT. However, in contrast to these two similarity-based methods, Multi-SKAT is multivariate regression based and hence provides a natural way to adjust for covariates and also can account for sample relatedness by incorporating random effects for the kinship matrix. Many of the existing methods for multiple-phenotype rare-variant tests can be viewed as special cases of Multi-SKAT with particular choices of kernels. Furthermore, to avoid loss of power due to model misspecification, we develop computationally efficient omnibus tests, which allow for aggregation of tests over several kernels and provide fast P value calculation (Demarta & McNeil, 2005).

The article is organized as follows: In the first section, we present the multivariate mixed effect model and kernel matrices. We particularly focus on the phenotype kernel and describe omnibus procedures that can aggregate results across different choices of kernels and kinship adjustment. In the next section, we describe the simulation experiments that clearly demonstrate that Multi-SKAT tests have increased power to detect associations compared with existing methods, like GAMuT, MSKAT, and others in most of the scenarios. Further, we applied Multi-SKAT to detect the cross-phenotype effects of rare nonsynonymous and protein-truncating variants on a set of nine amino acids measured on 8,545 Finnish men from the METSIM study.

2 | MATERIALS AND METHODS

2.1 | Single-phenotype region-based tests

To describe the Multi-SKAT tests, we first present the existing model of the single-phenotype gene or region-based tests. Let $y_k = (y_{1k}, y_{2k}, ..., y_{nk})^T$ be an $n \times 1$ vector of the kth phenotype over n individuals; X an $n \times q$ matrix of the q nongenetic covariates, including the intercept; $G_j = (G_{1j}, ..., G_{nj})^T$ is an $n \times 1$ vector of the minor allele counts (0, 1, or 2) for a binary genetic variant j; and $G = [G_1, ..., G_m]$ is an $n \times m$ genotype matrix for m

genetic variants in a target region. The regression model shown in Equation (1) can relate m genetic variants to phenotype k:

$$y_k = X\alpha_k + G\beta_k + \epsilon_k, \tag{1}$$

where α_k is a $q \times 1$ vector of regression coefficients of q nongenetic covariates, $\beta_k = (\beta_{1k},...,\beta_{mk})^T$ an $m \times 1$ vector of regression coefficients of the m genetic variants, and ϵ_k an $n \times 1$ vector of nonsystematic error term with each element following $N(0, \sigma_k^2)$. To test for $H_0: \beta_k = 0$, a variance component test under the mixed effect model has been proposed to increase power over the usual F test (Wu et al., 2011). The variance component test assumes that the regression coefficients, β_k, are random variables and follow a centered distribution with variance $\tau^2 \Sigma_G$ (see below). Under these assumptions, the test for $\beta_k = 0$ is equivalent to testing $\tau = 0$. The score statistic for this test is

$$Q = (y_k - \hat{\mu}_k)^T G \Sigma_G G^T (y_k - \hat{\mu}_k), \tag{2}$$

where $\hat{\mu}_k = X\hat{\alpha}_k$ is the estimated mean of y_k under the null hypothesis of no association. The test statistic Q asymptotically follows a mixture of X^2 distributions under the null hypothesis and P values can be computed by inverting the characteristic function (Davies, 1980).

The kernel matrix Σ_G plays a critical role; it models the relationship among the effect sizes of the variants on the phenotypes. Any positive semidefinite matrix can be used for Σ_G providing a unified framework for the region-based tests. A frequent choice of Σ_G is a sandwich-type matrix $\Sigma_G = W R_G W$, where $W = \text{diag}(w_1,...,w_m)$ is a diagonal weighting matrix for each variant, and R_G is a correlation matrix between the effect sizes of the variants. $R_G = I_{m \times m}$ implies uncorrelated effect sizes and corresponds to SKAT, and $R_G = 1_m 1_m^T$ corresponds to the Burden test, where $I_{m \times m}$ is an $m \times m$ diagonal matrix and $1_m = (1,...,1)^T$ is an $m \times 1$ vector with all elements being unity. Furthermore, a linear combination of these two matrices corresponds to $R_G = \rho 1_m 1_m^T + (1 - \rho) I_{m \times m}$, which is used for SKAT-O (Lee, Wu et al., 2012).

2.2 | Multiple-phenotype region-based tests

Extending the idea of using kernels, we build a model for multiple phenotypes. The multivariate linear model shown in Equation (3) can relate genetic variants to K-correlated phenotypes:

$$Y = XA + GB + E, \tag{3}$$

where $Y = (y_1,...,y_K)$ is an $n \times K$ phenotype matrix, A a $q \times K$ matrix of coefficients of X, $B = (\beta_{ij})$ an $m \times K$ matrix of coefficients, where β_{ij} denotes the effect of the ith variant on the jth phenotype, and E an $n \times K$ matrix of nonsystematic errors. Let $\text{vec}(\cdot)$ denote the matrix vectorization function, and then $\text{vec}(E)$ follows $N(0, I_n \otimes V)$, where V is a $K \times K$ covariance matrix and $\otimes$ represents the Kronecker product.

In addition to assuming that β_k follows a centered distribution with covariance $\tau^2 \Sigma_G$, we further assume that $\beta_{i.} = (\beta_{i1},...,\beta_{iK})^T$, which is the vector of regression coefficients of variant i for K multiple phenotypes, follows a centered distribution with covariance $\tau^2 \Sigma_P$, which implies that $\text{vec}(B)$ follows a centered distribution with covariance $\tau^2 \Sigma_G \otimes \Sigma_P$. As before, the null hypothesis $H_0: \text{vec}(B) = 0$ is equivalent to $\tau = 0$. The corresponding score test statistic is

$$Q = \{\text{vec}(Y) - \text{vec}(\hat{\mu})\}^T \{(G \Sigma_G G^T) \\ \otimes (\widehat{V}^{-1} \Sigma_P \widehat{V}^{-1})\} \{\text{vec}(Y) - \text{vec}(\hat{\mu})\}, \tag{4}$$

where $\hat{\mu}$ and $\widehat{V}$ are the estimated mean and covariance of Y under the null hypothesis.

Σ_P plays a similar role as Σ_G but with respect to phenotypes. Σ_P represents a kernel in the phenotypes space and models the relationship among the effect sizes of a variant on each of the phenotypes. Any positive semidefinite matrix can be used as Σ_P.

The proposed approach provides a double flexibility in modeling. Through the choice of structures for Σ_G and Σ_P, we can control the dependencies of genetic effects. Additionally, similar to SKAT, the use of a sandwich-type matrix $W R_G W$ for Σ_G allows us to upweight rare variants by using $\beta(1, 25)$ weights as in Wu et al. (2011). Most of our hypotheses about the underlying genetic structure of a set of phenotypes can be modeled through varying structures of these two matrices.

2.3 | Phenotype kernel structure Σ_P

The use of Σ_G has been extensively studied previously in the literature (Lee, Emond et al., 2012; Lee, Wu, et al., 2012; Wu et al., 2011). Here, we propose several choices for Σ_P and study their effect from a modeling perspective.

2.3.1 | Homogeneous (Hom) kernel

It is possible that effect sizes of a variant on different phenotypes are homogeneous, in which case $\beta_{j1} = \cdots = \beta_{jK}$. Under this assumption,

$$\Sigma_{P,\text{Hom}} = 1_K 1_K^T. \tag{5}$$

Under $\Sigma_{P,\text{Hom}}$, the effect sizes $\beta_{jk}, (k = 1, ..., K)$ for a variant j are the same for all the phenotypes.

2.3.2 | Heterogeneous (Het) kernel

Effect sizes of a variant on different phenotypes can be heterogeneous, in which $\beta_{j1} \neq \cdots \neq \beta_{jK}$. Under this assumption, we can construct

$$\Sigma_{P,\text{Het}} = I_{k\times k}. \tag{6}$$

The $\Sigma_{P,\text{Het}}$ implies that the effect sizes $(\beta_{j1}, ..., \beta_{jK}^T)$ are uncorrelated among themselves. This also indicates that the correlation among the phenotypes is not affected by this particular region or gene.

2.3.3 | Phenotype covariance (PhC) kernel

We may model Σ_P as proportional to the estimated residual covariance across the phenotypes as

$$\Sigma_{P,\text{PhC}} = \widehat{V}, \tag{7}$$

where $\widehat{V}$ is the estimated covariance matrix among the phenotypes. This model assumes that the correlation between the effect sizes is proportional to that between the residual phenotypes after adjusting for the nongenetic covariates.

2.3.4 | Principal component (PC) kernel

Principal component analysis (PCA) is a popular tool for multivariate analysis. In multiple-phenotype tests, PC-based approaches have been used to reduce the dimension in phenotypes (Aschard et al., 2014). Here, we show that PC-based approach can be included in our framework. Let $L = (L_1, ..., L_K)$ be the loading matrix with each column L_i produces the ith PC score. In Appendix A, we show that using $\Sigma_{P,\text{PC}} = \widehat{V} L \widehat{V}_P^{-1} \widehat{V}_P^{-1} L^T \widehat{V}$ is equivalent to assuming heterogeneous effects with all PCs as phenotypes. Instead of using all the PCs, we can use selected PCs that represent the majority of cumulative variations in phenotypes. For example, we can jointly test the PCs that have cumulative variance of 90%. If the top t PCs have been chosen for analysis using $\nu\%$ cumulative variance as cutoff, we can use

$$\Sigma_{P,\text{PC}-\nu} = \widehat{V} L_{\text{sel}} \widehat{V}_P^{-1} \widehat{V}_P^{-1} L_{\text{sel}}^T \widehat{V},$$

where $L_{\text{sel}} = [L_1, ..., L_t, 0, ..., 0]$ and 0 represents a vector of 0's of appropriate length.

2.3.5 | Relationship with other multiple-phenotype rare-variant tests

We have proposed a uniform framework of Multi-SKAT tests that depend on Σ_G and Σ_P. There are certain specific choices of kernels that correspond to other published methods.

- Using $\Sigma_{P,\text{PhC}}$ and $\Sigma_G = WI_mW^T$ is identical to the GAMuT (Broadaway et al., 2016) with the projection phenotype kernel and the MSKAT with the Q statistic (Wu & Pankow, 2016).
- Using $\Sigma_P = \widehat{V}^2$ and $\Sigma_G = WI_mW^T$ is identical to GAMuT (Broadaway et al., 2016) with the linear phenotype kernel and the MSKAT with the Q' statistic (Wu & Pankow, 2016).
- Using $\Sigma_{P,\text{Hom}}$ and $\Sigma_G = WI_mW^T$ is identical to hom-MAAUSS (Lee et al., 2016).
- Using $\Sigma_{P,\text{Het}}$ and $\Sigma_G = WI_mW^T$ is identical to het-MAAUSS (Lee et al., 2016) and MF-KM (Yan et al., 2015).

For the detailed proof, please see Appendix B.

2.4 | Minimum P value-based omnibus tests (minP and minP$_{\text{com}}$)

The model and the corresponding test of association that we propose have two parameters, Σ_G and Σ_P, which are absent in the null model of no association. Because our test is a score test, Σ_G and Σ_P cannot be estimated from the data. One possible approach is to select Σ_G and Σ_P based on prior knowledge; however, if the selected Σ_G and Σ_P do not reflect underlying biology, the test may have substantially reduced power (Lee et al., 2016; Ray et al., 2016). In an attempt to achieve robust power, we aggregate results across different Σ_G and Σ_P using the minimum of P values from different kernels.

Although this omnibus test approach has been used in rare-variant tests and multiple-phenotype analyses for combining multiple kernels from genotypes and phenotypes (He, Xu, Lee, & Ionita-Laza, 2017; Urrutia et al., 2015; Wu, Maity, Lee, & Simmons, 2013; Zhan et al., 2017), it is challenging to calculate the P value, because the minimum P value does not follow the uniform distribution. One possible approach is using permutation or perturbation to calculate the Monte-Carlo P value (Urrutia et al., 2015; Zhan et al., 2017); however, this approach is computationally too expensive to be used in genome-wide analysis. To address it, here we propose a fast Copula-based P value calculation for Multi-SKAT, which needs only a small number of resampling steps to calculate the P value.

Suppose p_h is the P value for Q_h with given hth Σ_G and Σ_P, $h = 1,...,b$, and $T_P = (p_1,...,p_b)^T$ is a $b \times 1$ vector of P values of b such Multi-SKAT tests. The minimum P value test statistic after the Bonferroni adjustment is $b \times p_{min}$, where p_{min} is the minimum of the b P values. In the presence of positive correlation among the tests, this approach is conservative and hence might lack power of detection. Rather than using the Bonferroni-corrected p_{min}, more accurate results can be obtained if the joint null distribution or more specifically the correlation structure of T_P can be estimated. Here, we adopt a resampling-based approach to estimate this correlation structure. Note that our test statistic is equivalent to

$$Q = S^T \left\{ (G\Sigma_G G^T) \otimes \left(\widehat{V}^{-\frac{1}{2}} \Sigma_P \widehat{V}^{-\frac{1}{2}} \right) \right\} S, \qquad (8)$$

where $S = (I_n \otimes \widehat{V}^{-\frac{1}{2}})\{vec(Y) - vec(\widehat{\mu})\}$. Under the null hypothesis, S approximately follows an uncorrelated normal distribution $N(0, I_{nK})$. Using this, we propose the following resampling algorithm:

1. Generate nK samples from an $N(0, 1)$ distribution, say S_R.
2. Calculate b different test statistics as $Q_R = S_R^T \{(G\Sigma_G G^T) \otimes (\widehat{V}^{-\frac{1}{2}} \Sigma_P \widehat{V}^{-\frac{1}{2}})\} S_R$ for all the choices of Σ_P and calculate P values.
3. Repeat the previous steps independently for $R(=1,000)$ iterations and calculate the correlation between the P values of the tests from the R resampling P values.

With the estimated null-correlation structure, we use a Copula to approximate the joint distribution of T_P (Demarta & McNeil, 2005; He et al., 2017). Copula is a statistical approach to construct joint multivariate distribution using marginal distribution of each variable and correlation structure. Because marginally each test statistic Q follows a mixture of X^2 distributions, which has a heavier tail than normal distribution, we propose to use a t-Copula to approximate the joint distribution, that is, we assume the joint distribution of T_P to be multivariate t with the estimated correlation structure. The final P value for association is then calculated from the distribution function of the assumed t-Copula.

When calculating the correlation across the P values, Pearson's correlation coefficient can be unreliable because it depends on normality and homoscedasticity assumptions. To avoid such assumptions, we recommend estimating the null-correlation matrix of the P values through Kendall's tau (τ), which is a nonparametric approach based on concordance of ranks.

The minimum P value approach can be used to combine different Σ_P's given Σ_G, or combine both Σ_P and Σ_G. For example, two Σ_G's corresponding to SKAT (WW) and Burden kernels ($W1_m 1_m^T W$) and four Σ_P's ($\Sigma_{P,Hom}$, $\Sigma_{P,Het}$, $\Sigma_{P,PhC}$, and $\Sigma_{P,PC-0.9}$) can be combined, which results in the omnibus test of these eight different tests. To differentiate the latter, we will call it minP$_{com}$, which combines SKAT and Burden-type kernels of Σ_G.

2.5 | Adjusting for relatedness

We formulated Equation (3) and corresponding tests under the assumption of independent individuals. If individuals are related, this assumption is no longer valid, and the tests may have inflated Type I error rate. Because our method is regression based, we can relax the independence assumption by introducing a random effect term to account for the relatedness among individuals.

Let Φ be the kinship matrix of the individuals and V_g is a coheritability matrix, denoting the shared heritability between the phenotypes. Extending the model presented in Equation (3), we incorporate Φ and V_g as

$$Y = XA + GB + Z + E, \qquad (9)$$

where Z is an $n \times K$ matrix with $vec(Z)$ following $N(0, \Phi \otimes V_g)$. Z represents a matrix of random effects arising from shared genetic effects between individuals due to the relatedness. The remaining terms are the same as in Equation (3). The corresponding score test statistic is

$$Q_{Kin} = S_{Kin}^T \widehat{V}_e^{-1/2} \{(G\Sigma_G G^T) \otimes \Sigma_P\} \widehat{V}_e^{-1/2} S_{Kin}, \quad (10)$$

where $S_{Kin} = \widehat{V}_e^{-1/2}\{vec(Y) - vec(\widehat{\mu})\}$ and $\widehat{V}_e = \Phi \otimes \widehat{V}_g + I_n \otimes \widehat{V}$ is the estimated covariance matrix of $vec(Y)$ under the null hypothesis. Similar to the previous versions for unrelated individuals, Q_{Kin} asymptotically follows a mixture of X^2 under the assumption of no association.

This approach depends on the estimation of the matrices Φ, V_g, and V. The kinship matrix Φ can be estimated using the genome-wide genotype data (Manichaikul et al., 2010). Several of the published methods, like LD-Score (Bulik-Sullivan et al., 2015), phenotype imputation expedited (PHENIX) (Dahl et al., 2016), and genome-wide efficient mixed model association (GEMMA) (Zhou & Stephens, 2014; Zhou, Carbonetto, & Matthew, 2013) can jointly estimate V_g and V. In our numerical analysis, we have used PHENIX. This is an efficient method to fit local maximum likelihood variance components in a multiple-phenotype-mixed model through an E–M algorithm.

Once the matrices Φ, V_g, and V are estimated, we compute the asymptotic P values for Q_{Kin} by using a

mixture of X^2 distribution. The computation of $Q_{K\text{in}}$ requires large matrix multiplications, which can be time and memory consuming. To reduce computational Burden, we employ several transformations. We perform an eigen decomposition on the kinship matrix Φ as $\Phi = U\Lambda U^T$, where U is an orthogonal matrix of eigenvectors and Λ is a diagonal matrix of corresponding eigenvalues. We obtain the transformed phenotype matrix as $\widetilde{Y} = U'Y$, the transformed covariate matrix as $\widetilde{X} = U'X$, the transformed random effects matrix $\widetilde{Z} = U'Z$ and transformed residual error matrix $\widetilde{E} = U'E$. Equation (9) can be transformed into

$$\widetilde{Y} = \widetilde{X}A + \widetilde{G}B + \widetilde{Z} + \widetilde{E}, \qquad \text{vec}(\widetilde{Z}) \sim N(0, \Lambda \otimes V_g),$$
$$\text{vec}(\widetilde{E}) \sim N(0, I \otimes V). \qquad (11)$$

All the properties of the tests developed from Equation (3) are directly applicable to those from Equation (11). $Q_{K\text{in}}$ can be computed from this transformed equation as

$$Q_{K\text{in}} = \widetilde{S}_{K\text{in}}^T \widetilde{V}_e^{-1/2} \{(\widetilde{G}\Sigma_G \widetilde{G}^T) \otimes \Sigma_P\} \widetilde{V}_e^{-1/2} \widetilde{S}_{K\text{in}}, \quad (12)$$

where $\widetilde{S}_{K\text{in}} = \widetilde{V}_e^{-1/2}\{\text{vec}(\widetilde{Y}) - \text{vec}(\widetilde{\mu})\}$, $\widetilde{\mu}$ is the estimated mean of $\widetilde{Y}$ under the null hypothesis and $\widetilde{V}_e = \Lambda \otimes \widehat{V}_g + I_n \otimes \widehat{V}$. Asymptotic P values can be obtained from the corresponding mixture of X^2 distribution. Further, omnibus strategies for the tests developed from Equation (3) are applicable in this case with similar modifications. For example, the resampling algorithm for minimum P value-based omnibus test can be implemented here as well by noting that $\widetilde{S}_{K\text{in}}$ approximately follows an uncorrelated normal distribution.

3 | SIMULATIONS

We carried out extensive simulation studies to evaluate the Type I error control and power of Multi-SKAT tests. For Type I error simulations without related individuals and all power simulations, we generated 10,000 chromosomes over 1 Mbp regions using a coalescent simulator with the European demographic model (Schaffner et al., 2005). The minor allele frequency (MAF) spectrum of the simulated variants is shown in Supporting Information Figure S6, showing that most of the variants are rare variants. Because the average length of the gene is 3 kbps, we randomly selected a 3-kbps region for each simulated data set to test for associations. For the Type I error simulations with related individuals, to have a realistic kinship structure, we used the METSIM study genotype data.

Phenotypes were generated from the multivariate normal distribution as

$$y_i \sim \text{MVN}\{(\beta_1 G_1 + \cdots + \beta_m G_m)I, V\}, \qquad (13)$$

where $y_i = (y_{i1},...,y_{iK})^T$ is the outcome vector, G_j the genotype of the jth variant, and β_j the corresponding effect size, and V a covariance of the nonsystematic error term. We use V to define level of covariance between the traits. I is a $k \times 1$ indicator vector, which has 1 when the corresponding phenotype is associated with the region and 0 otherwise. For example, if there are five phenotypes and the last three are associated with the region, $I = (0, 0, 1, 1, 1)^T$.

To evaluate whether Multi-SKAT can control Type I error under realistic scenarios, we simulated a data set with nine phenotypes with a correlation structure identical to that of nine amino acid phenotypes in the METSIM data (see Supporting Information Figure S1). Phenotypes were generated using Equation (13) with $\beta = 0$. Total 5,000,000 data sets with 5,000 individuals were generated to obtain the empirical Type I error rates at $\alpha = 10^{-4}$, 10^{-5}, and 2.5×10^{-6}, which are corresponding to candidate gene studies to test for 500 and 5,000 genes and exome-wide studies to test for all 20,000 protein coding genes, respectively.

Next, we evaluated Type I error controls in the presence of related individuals. To have a realistic related structure, we used the METSIM study genotype data. We generated a random subsample of 5,000 individuals from the METSIM study individuals and generated null values for the nine phenotypes from $\text{MVN}(0, V_e)$, where $V_e = \Phi_{5k} \otimes \widehat{V}_{g;5k} + I \otimes \widehat{V}_{5k}$, Φ_{5k} is the estimated kinship matrix of the 5,000 selected individuals, $\widehat{V}_{g;5k}$ and $\widehat{V}_{5k}$ are estimated coheritability and residual variance matrices, respectively, for these individuals as estimated using the multiple phenotype mixed model (MPMM) function in the PHENIX R-package (version 1.0 See Web Resources). For each set of nine phenotypes, we performed the Multi-SKAT tests for randomly selected 5,000 genes in the METSIM data. For the details about the data, see the next section. We carried out this procedure 1,000 times and obtained 5, 000, 000 P values and estimated Type I error rate as proportions of P values smaller than the given level α.

Our simulation studies focus on evaluating the power of the proposed tests when the number of phenotypes is five or six. Power simulations were performed both in situations when there was no pleiotropy (i.e., only one of the phenotypes was associated with the causal variants) and also when there was pleiotropy. Under pleiotropy, because it is unlikely that all the phenotypes are associated with genotypes in the region, we varied the number of phenotypes associated. For each associated phenotype, 30% or 50% of the rare variants (MAF < 1%) was randomly selected to be causal variants. We modeled the rarer variants to have stronger effect, as $|\beta_j| = c|\log_{10}(\text{MAF}_j)|$. We used $c = 0.3$,

which yields $|\beta_j| = 0.9$ for variants with MAF $= 10^{-3}$. Our choice of β yielded the average heritability of associated phenotypes between 1% and 4%. We also considered situations that all causal variants were trait-increasing variants (i.e., positive β) or 20% of causal variants was trait-decreasing variants (i.e., negative β). Empirical power was estimated from 1,000 independent data sets at exome-wide $\alpha = 2.5 \times 10^{-6}$.

In Type I error and power simulations, we compared the following tests:

- Bonferroni-adjusted minimum P values from gene-based test (SKAT, Burden, or SKAT-O) on each phenotype (minPhen),
- Multi-SKAT with $\Sigma_{P,\text{Hom}}$ (Hom),
- Multi-SKAT with $\Sigma_{P,\text{Het}}$ (Het),
- Multi-SKAT with $\Sigma_{P,\text{PhC}}$ (PhC),
- Multi-SKAT with $\Sigma_{P,\text{PC}-0.9}$ (PC-Sel),
- Minimum P value of Hom, Het, PhC, and PC-Sel using Copula (minP),
- Minimum P value of Hom, Het, PhC, and PC-Sel with Σ_G being SKAT and Burden, using Copula (minP$_{\text{com}}$).

For the Multi-SKAT tests, we used two different Σ_G's corresponding to SKAT (i.e., $\Sigma_G = WW$) and Burden tests (i.e., $\Sigma_G = W1_m 1_m^T W$). For the variant weighting matrix $W = \text{diag}(w_1,...,w_m)$, we used $w_j = \beta(\text{MAF}_j, 1, 25)$ function to upweight rarer variants, as recommended by Wu et al. (2011).

3.1 | Computation time

We estimated the computation time of Multi-SKAT tests and the existing methods. Using simulated data sets of 5,000 related and unrelated individuals with 10 phenotypes and 20 genetic variants, we estimated the computation time of Multi-SKAT tests with and without kinship adjustments. To compare the computation performance of Multi-SKAT tests with the existing methods, we generated data sets of unrelated individuals with five different sample sizes ($n = 1,000$, 2,000, 10,000, 15,000, and 20,000) and four different number of variants ($m = 10$, 20, 50, and 100). For each simulation setup, we generated 100 data sets and obtained the average value of the computation time.

3.2 | Analysis of the METSIM study ExomeChip data

To investigate the cross-phenotype roles of low frequency and rare variants on amino acids, we analyzed data on 8,545 participants of the METSIM study on whom all nine amino acids (alanine, leucine, isoleucine, glycine, valine, tyrosine, phenylalanine, glutamine, and histidine) were measured by proton nuclear magnetic resonance

spectroscopy (Teslovich et al., 2018). Individuals were genotyped on the Illumina ExomeChip and OmniExpress arrays, and we included individuals that passed sample quality control filters (Huyghe et al., 2013). The kinship between the individuals was estimated via KING (version 2.0; Manichaikul et al., 2010, See Web Resources). We adjusted the amino acid levels for age, age^2, and BMI and inverse normalized the residuals. The phenotype correlation matrix after covariate adjustment is shown in Figure 3 and Supporting Information Figure S1. Subsequently, we estimated the genetic heritability matrix and the residual covariance matrix using the MPMM function from PHENIX R-package (Dahl et al., 2016).

We included rare (MAF < 1%) nonsynonymous and protein-truncating variants with a total rare minor allele count of at least five for genes that had at least three rare variants leaving 5,207 genes for analysis. We set a stringent significance threshold at 9.6×10^{-6} corresponding to the Bonferroni adjustment for 5,207 genes. Further, we also considered a less stringent threshold of 10^{-4}, corresponding to a candidate gene study of 500 genes, as suggestive to study the associations, which were not significant but close to the threshold.

4 | RESULTS

4.1 | Type I error simulations

We estimated empirical Type I error rates of the Multi-SKAT tests with and without related individuals. For unrelated individuals, we simulated 5,000 individuals and nine phenotypes based on the correlation structure for the amino acid phenotypes in the METSIM study data. For related individuals, we simulated 5,000 individuals using the kinship matrix for randomly chosen METSIM individuals (see Section 2). We performed association tests and estimated Type I error rate as the proportion of P values less than the specified α levels. Type I error rates of the Multi-SKAT tests were well maintained at $\alpha = 10^{-4}$, 10^{-5}, and 2.5×10^{-6} for both unrelated and related individuals (Table 1), which correspond to candidate gene studies of 500 and 5,000 genes and exome-wide studies to test for all 20,000 protein coding genes, respectively. For example, at level $\alpha = 2.5 \times 10^{-6}$, the largest empirical Type I error rate from any of the Multi-SKAT tests was 3.4×10^{-6}, which was within the 95% confidence interval (CI = $[1.6 \times 10^{-6}, 4 \times 10^{-6}]$).

4.2 | Power simulations

We compared the empirical power of the minPhen (Bonferroni-adjusted minimum P value for the

TABLE 1 Empirical Type I error rates of the Multi-SKAT tests from 5,000,000 simulated null data sets

Level	Σ_G	minPhen	Hom	Het	PhC	PC-Sel	minP	minP$_{com}$
Independent samples (without kinship adjustment)								
	SKAT	2.4×10^{-06}	2.6×10^{-06}	2.6×10^{-06}	2.8×10^{-06}	2.6×10^{-06}	3.4×10^{-06}	
2.5×10^{-06}								2.8×10^{-06}
	Burden	2.4×10^{-06}	2.8×10^{-06}	2.6×10^{-06}	2.6×10^{-06}	2.6×10^{-06}	3.0×10^{-06}	
	SKAT	9.6×10^{-06}	9.6×10^{-06}	9.8×10^{-06}	9.8×10^{-06}	9.8×10^{-06}	9.4×10^{-06}	
10^{-05}								1.2×10^{-05}
	Burden	9.4×10^{-06}	9.6×10^{-06}	9.8×10^{-06}	9.6×10^{-06}	9.6×10^{-06}	9.6×10^{-06}	
	SKAT	9.6×10^{-05}	9.4×10^{-05}	9.6×10^{-05}	9.8×10^{-05}	9.8×10^{-05}	9.8×10^{-05}	
10^{-04}								1.1×10^{-04}
	Burden	9.8×10^{-05}	9.6×10^{-05}	9.4×10^{-05}	9.7×10^{-05}	9.6×10^{-05}	9.7×10^{-05}	
Related samples (with kinship adjustment)								
	SKAT	2.2×10^{-06}	2.4×10^{-06}	2.4×10^{-06}	2.8×10^{-06}	2.6×10^{-06}	3.0×10^{-06}	
2.5×10^{-06}								2.6×10^{-06}
	Burden	2.2×10^{-06}	2.6×10^{-06}	2.4×10^{-06}	2.6×10^{-06}	2.4×10^{-06}	3.2×10^{-06}	
	SKAT	9.6×10^{-06}	9.8×10^{-06}	9.8×10^{-06}	9.8×10^{-06}	9.8×10^{-06}	9.4×10^{-06}	
10^{-05}								1.4×10^{-05}
	Burden	9.7×10^{-06}	9.6×10^{-06}	9.4×10^{-06}	9.4×10^{-06}	9.4×10^{-06}	9.4×10^{-06}	
	SKAT	9.4×10^{-05}	9.6×10^{-05}	9.7×10^{-05}	9.8×10^{-05}	9.4×10^{-05}	9.8×10^{-05}	
10^{-04}								1.2×10^{-04}
	Burden	9.5×10^{-05}	9.7×10^{-05}	9.6×10^{-05}	9.8×10^{-05}	9.8×10^{-05}	9.7×10^{-05}	

Note. Het: heterogeneous; Hom: homogeneous; METSIM: METabolic Syndrome In Men; minP: minimum P value; PC: principal component; PhC: phenotype covariance.
The number of phenotypes was nine, and the correlation structure among the phenotypes was similar to that of the amino acid phenotypes in the METSIM study data. The sample size was 5,000.

phenotypes) and Multi-SKAT tests. For each simulation setting, we generated 1,000 sequence data sets of 5,000 unrelated individuals and for each test estimated empirical power as the proportion of P values less than $\alpha = 2.5 \times 10^{-6}$, reflecting the Bonferroni correction for testing 20,000 independent genes. Because the Hom and Het tests are identical to hom-MAAUSS and het-MAAUSS, respectively, and using PhC is identical to both GAMuT (with projection phenotype kernel) and MSKAT, our power simulation studies effectively compare the existing multiple-phenotype tests.

In Figure 1, we show the results for five phenotypes with compound symmetric correlation structure with the correlation 0.3 or 0.7, where 30% of rare variants (MAF < 0.01) was positively associated with 1, 2, or 3 phenotypes. Because it is unlikely that all the phenotypes are associated with the region, we restricted the number of associated phenotypes to at most 3. In most scenarios, PhC, PC-Sel, and Het had greater power among the Multi-SKAT tests with fixed phenotype kernels (i.e., Hom, Het, PhC, and PC-Sel), whereas minP maintained high power as well. For example,

when the correlation between the phenotypes was 0.3 (i.e., $\rho = 0.3$) and the SKAT kernel was used for the genotype kernel Σ_G, if three phenotypes were associated with the region, minP and PhC were more powerful than that of the other tests. If the correlation between the phenotypes was $\rho = 0.7$ and the Burden kernel was used for genotype kernel Σ_G, Het, PC-Sel, and minP had higher power than the rest of the tests when two phenotypes were associated. It is noteworthy that Hom had the lowest power in all the scenarios of Figure 1.

Figure 2 demonstrates scenarios involving six phenotypes and clustered correlation structures where PhC was outperformed by other choices of the phenotype kernel Σ_P. When all three phenotype clusters had associated phenotypes and the correlation within the clusters was low ($\rho = 0.3$; Figure 2, upper panel), Hom and minP tests outperformed PhC when the SKAT kernel was used. This may be because that the phenotype correlation structure did not reflect the genetic association pattern. When two small clusters had high within-cluster correlation ($\rho = 0.7$) and one large cluster had low within-cluster
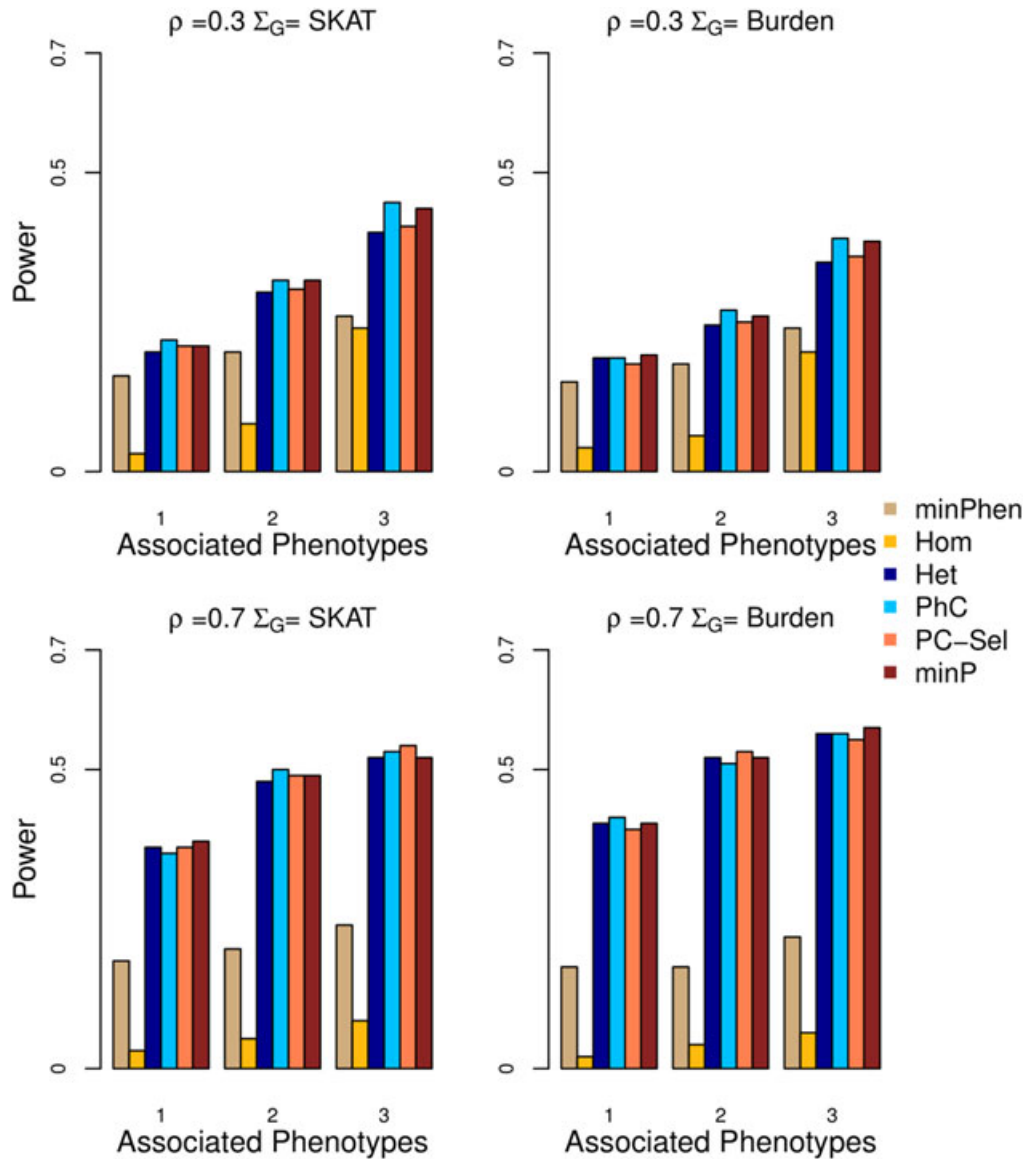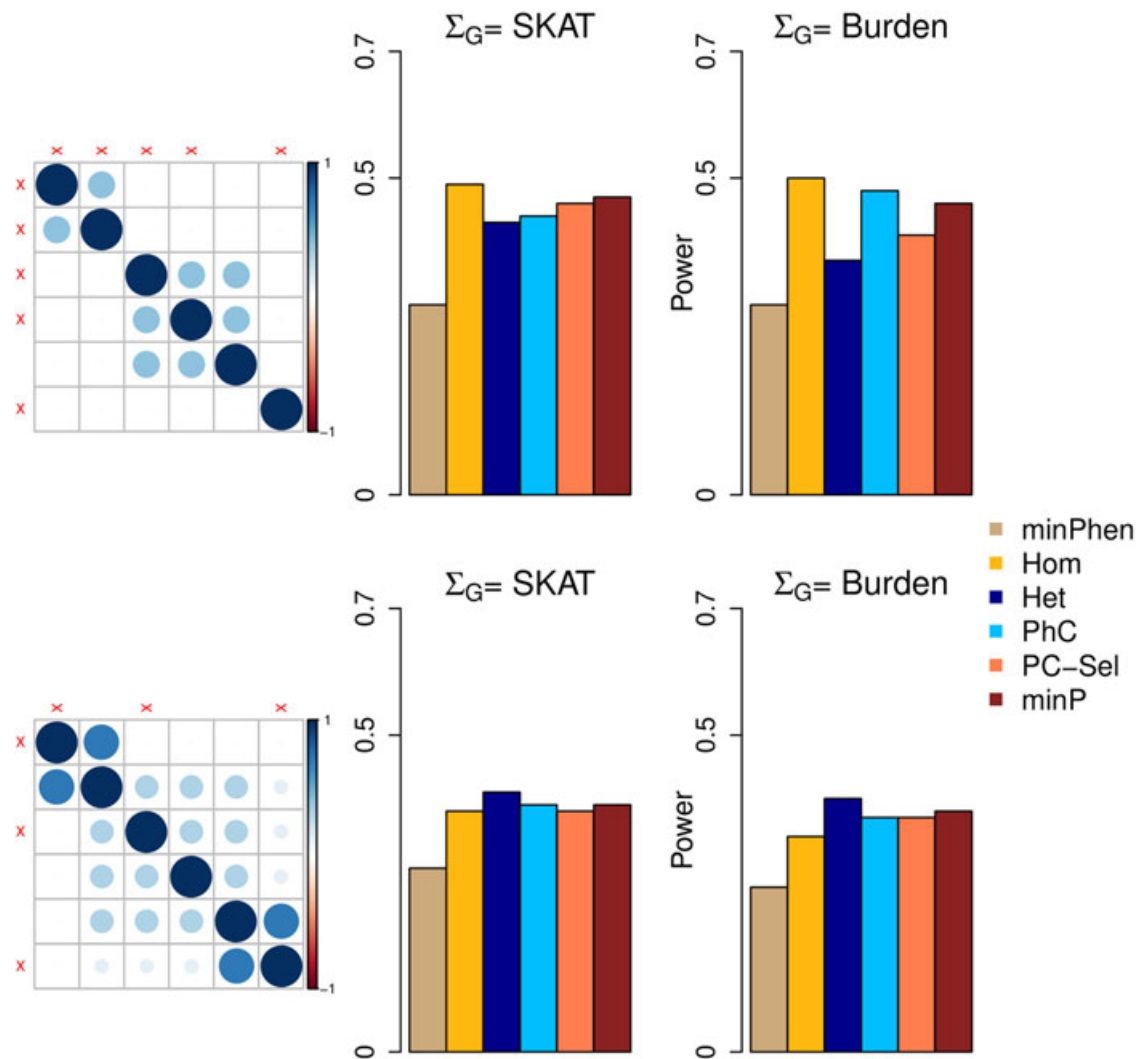
FIGURE 1 Power for Multi-SKAT tests when phenotypes have compound symmetric correlation structures. Empirical power for minPhen, Hom, Het, PhC, PC-Sel, and minP plotted against the number of phenotypes associated with the gene of interest with a total of five phenotypes under consideration. Upper row shows the results for $\rho = 0.3$ and lower row for $\rho = 0.7$. Left column shows the results with the SKAT kernel Σ_G, and right columns shows the results with the Burden kernel. All the causal variants were trait-increasing variants. Het: heterogeneous; Hom: homogeneous; minP: minimum P value; PC: principal component; PhC: phenotype covariance

correlation ($\rho = 0.3$; Figure 2, lower panel), Het and minP had higher power than PhC.

When 20% of causal variants was trait-decreasing variants (80% trait-increasing), the power of Multi-SKAT tests with Burden Σ_G was reduced (Supporting Information Figures S2 and S3). This is because the association signals were attenuated due to the mix of trait-increasing and trait-decreasing variants. Because SKAT is robust regardless of the association direction, power with SKAT Σ_G was largely maintained. The relative performance of methods with different Σ_P given Σ_G was quantitatively similar to the results without trait-decreasing variants.

Further, we estimated power of minP$_{com}$, which combines tests across phenotype (Σ_P) and genotype Σ_G kernels. The power of minP$_{com}$ was evaluated for the compound symmetric phenotype correlation structure presented in Figure 1 and was compared with the two minP tests of SKAT (minP-SKAT) and Burden (minP-Burden) Σ_G kernels. Figure 3 shows empirical power with and without trait-decreasing variants. When all genetic effect coefficients were positive (Figure 3, left panel), the performances of minP-SKAT and minP-Burden were similar for both the situations where the correlations between the phenotypes were low (i.e., $\rho = 0.3$) and high (i.e., $\rho = 0.7$). When

FIGURE 2 Power for Multi-SKAT tests when phenotypes have clustered correlation structures. Empirical powers for minPhen, Hom, Het, PhC, PC-Sel, and minP are plotted under different levels of association with a total of six phenotypes and with clustered correlation structures. Middle column shows the empirical powers for different combinations of phenotypes associated with the SKAT kernel Σ_G; the rightmost column shows the corresponding results with the Burden kernel; left column shows the corresponding correlation matrices for the phenotypes. The associated phenotypes are indicated in red cross marks across the correlation matrices. All the causal variants were trait-increasing variants. Het: heterogeneous; Hom: homogeneous; minP: minimum P value; PC: principal component; PhC: phenotype covariance

20% of genetic effect coefficients was negative (Figure 3, right panel), as expected, the power of minP-Burden was substantially decreased. Across all the situations, the power of $minP_{com}$ was similar to the most powerful minP with fixed genotype kernel Σ_G. When 50% of variants was causal variants and all genetic effect coefficients were positive (Supporting Information Figure S4, left panel), minP-Burden was more powerful than minP-SKAT, and $minP_{com}$ had similar power than minP-Burden.

Overall, our simulation results show that the omnibus tests, especially $minP_{com}$, had robust power throughout all the simulation scenarios considered. When Σ_G and Σ_P were fixed, power depended on the model of association and the correlation structure of the phenotypes. Overall,

the proposed Multi-SKAT tests generally outperformed the single-phenotype test (minPhen), even when only one phenotype was associated with genetic variants.

4.3 | Application to the METSIM study ExomeChip data

Inborn errors of amino acid metabolism cause mild to severe symptoms, including type 2 diabetes (Stančáková et al., 2012; Würtz et al., 2012, 2013) and liver diseases (Tajiri & Shimizu, 2013) among others. Amino acid levels are perturbed in certain disease states, for example, glutamic and aspartic acid levels are reduced in Alzheimer disease brains (Allan Butterfield & Pocernich,
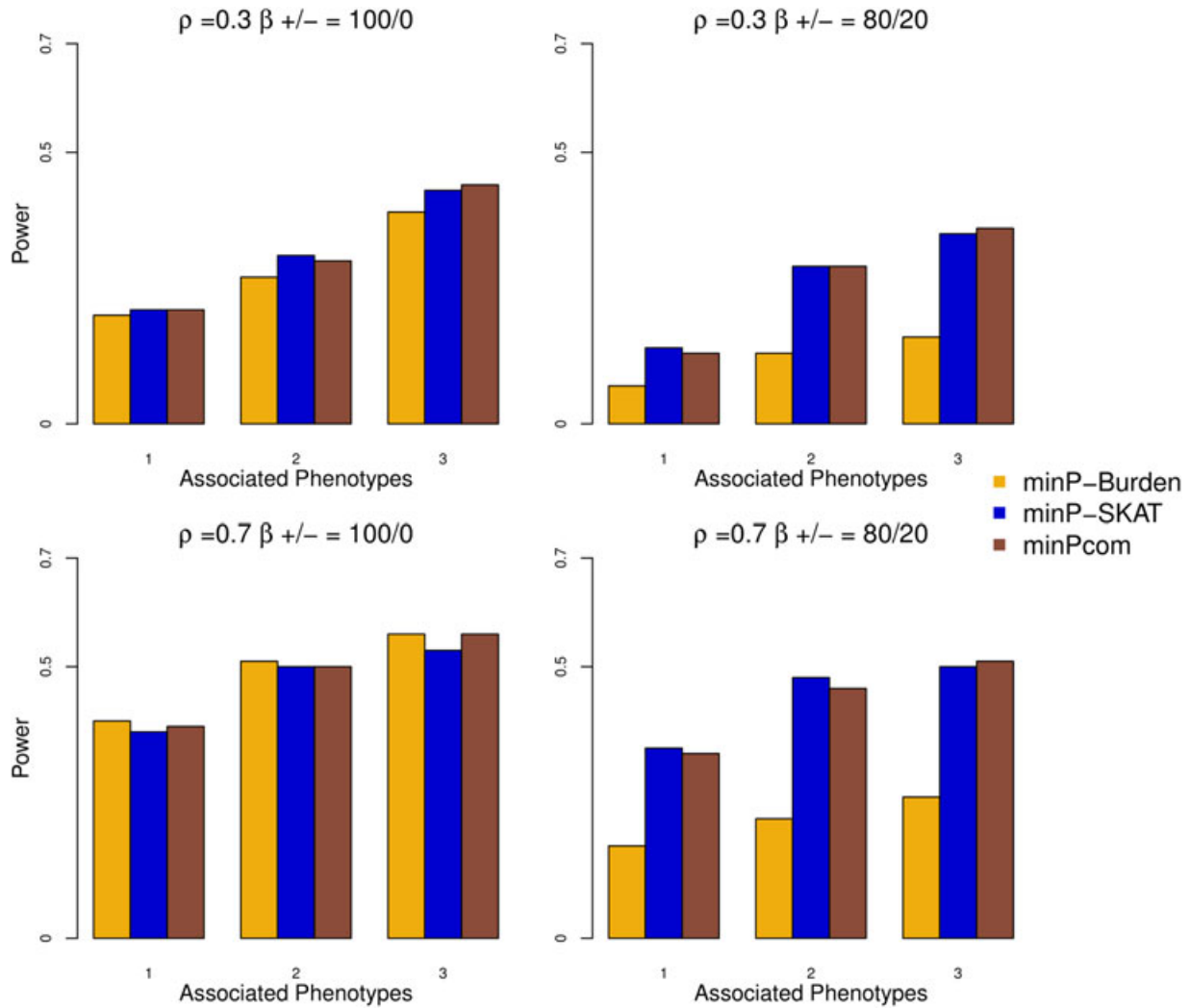
FIGURE 3 Power for Multi-SKAT by combining tests with Σ_P as Hom, Het, PhC, PC-Sel, and Σ_G as SKAT and Burden when phenotypes have compound symmetric correlation structures. Empirical powers for minP-Burden, minP-SKAT, and minP$_{com}$ are plotted against the number of phenotypes associated with the gene of interest with a total of five phenotypes under consideration. Upper row shows the results for $\rho = 0.3$ and lower row for $\rho = 0.7$. Left column shows the results when all the causal variants were trait-increasing variants, and right column shows the results when 80%/20% of the causal variants was trait-increasing/trait-decreasing variants. Het: heterogeneous; Hom: homogeneous; minP: minimum P value; PC: principal component; PhC: phenotype covariance

2003); isoleucine, glycine, alanine, phenylalanine, and threonine levels are increased in cerebo-spinal fluid (CSF) of individuals with motor neuron disease (de Belleroche & Recordati, 2003). To find rare variants associated with the nine measured amino acid levels, we applied the Multi-SKAT tests to the METSIM study data (Teslovich et al., 2018). The MAF spectrum of the genotyped variants is shown in Supporting Information Figure S6, showing that most of the variants are rare variants. We estimated the relatedness between individuals by KING (Manichaikul et al., 2010) and coheritability of the amino acid phenotypes and the corresponding residual variance using PHENIX (Dahl et al., 2016; Supporting Information Figure S1). Among the 8,545 METSIM participants with nonmissing pheno-

types and covariates, 1,332 individuals had a second degree or closer relationship with one or more of the METSIM participants. A total of 5, 207 genes with at least three rare variants were included in our analysis. The Bonferroni corrected significance threshold was $\alpha = 0.05/5207 = 9.6 \times 10^{-6}$. Further, we used a less significant cutoff of $\alpha = 10^{-4}$ for a gene to be suggestive. After identifying associated genes, we carried out backward elimination procedure (Appendix C) to investigate which phenotypes are associated with the gene. This procedure iteratively removes phenotypes based on minP$_{com}$ P values.

Quantile-quantile (QQ) plots for the P values obtained by minPhen and Multi-SKAT omnibus tests (minP and minP$_{com}$) are displayed in Figure 4. Due to the presence
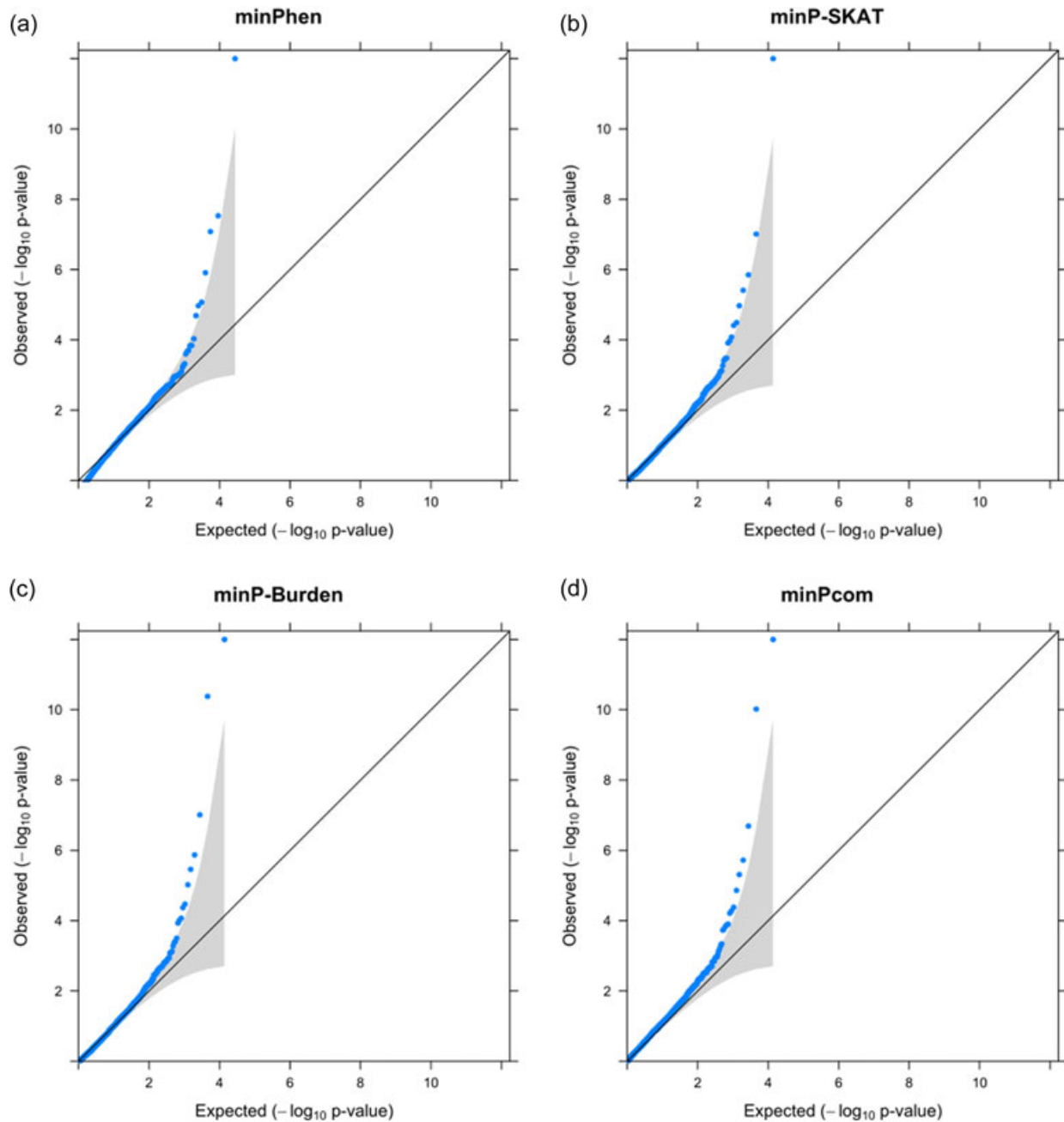
FIGURE 4 QQ plot of the *P* values of minPhen and Multi-SKAT omnibus tests for the METSIM data. For the ease of viewing, any associations with *P* values $< 10^{-12}$ have been collapsed to 10^{-12}. METSIM: METabolic Syndrome In Men; QQ: quantile quantile

of several strong associations, for the ease of viewing, any *P* value $< 10^{-12}$ was collapsed to 10^{-12}. The QQ plots are well calibrated with slight inflation in tail areas. The genomic-control lambda (λ_{GC}) varied between 0.97 and 1.04, which indicates no inflation of test statistics. Table 2 shows genes with *P* values less than 10^{-4} for minPhen or minP$_{com}$. Table 5 shows SKAT-O *P* values for each of the gene–amino acid pairs. Among the eight significant or suggestive genes displayed in Table 2, minP$_{com}$ provides more significant *P* values than minPhen for six genes:

Glycine decarboxylase (*GLDC* [MIM: 238300]), histidine ammonia-lyase (*HAL* [MIM: 609457]), phenylalanine hydroxylase (*PAH* [MIM: 612349]), dihydroorotate dehydrogenase (*DHODH* [MIM: 126064]), mediator of RNA polymerase II transcription subunit 1 (*MED1* [MIM: 604311]), and serine/threonine kinase 33 (*STK33* [MIM: 607670]). Interestingly, *PAH* and *MED1* are significant by minP$_{com}$, but not significant by minPhen. *PAH* encodes an phenylalanine hydroxylase, which catalyzes the hydroxylation of the aromatic side-chain of phenylalanine

TABLE 2 Significant and suggestive genes associated with nine amino acid phenotypes

Gene	Chromosome	Rare SNPs	MAC	minPhen	minP-SKAT	minP-Burden	minPcom
GLDC	9	4	183	2.2×10^{-63}	1.1×10^{-72}	9.7×10^{-64}	2.3×10^{-72}
HAL	3	6	42	2.9×10^{-08}	1.1×10^{-05}	4.2×10^{-11}	9.5×10^{-11}
DHODH	16	5	90	1.3×10^{-06}	9.7×10^{-08}	7.7×10^{-06}	1.1×10^{-07}
PAH	12	6	27	6.1×10^{-04}	1.4×10^{-06}	1.3×10^{-06}	1.9×10^{-06}
MED1	17	3	147	6.2×10^{-01}	3.9×10^{-06}	3.4×10^{-04}	4.9×10^{-06}
STK33	11	6	180	8.9×10^{-01}	3.2×10^{-05}	3.3×10^{-02}	4.2×10^{-05}
ALDH1L1	3	8	103	8.4×10^{-08}	3.8×10^{-04}	4.2×10^{-05}	5.4×10^{-05}
BCAT2	19	3	133	1.1×10^{-05}	9.3×10^{-03}	3.4×10^{-05}	6.2×10^{-05}

Note. MAF: minor allele frequency; minP: minimum *P* value using copula; SNP: single-nucleotide polymorphism; MAC: minor allele count.
Genes with *P* values < 10^{-4} by minPhen or any Multi-SKAT tests (minP-SKAT, minP-Burden, and minP$_{com}$) were reported in this table. Multi-SKAT tests were applied with the kinship adjustment, and 5,207 genes with at least three rare (MAF < 0.01) nonsynonymous and protein-truncating variants were used in this analysis. The total sample size was $n = 8,545$. *P* values smaller than the Bonferroni corrected significance $\alpha = 9.6 \times 10^{-6}$ were marked as bold. Smallest *P* values for each gene among all the tests have been underlined. minPhen was calculated as the Bonferroni-adjusted minimum SKAT-O *P* value across each phenotype.

to generate tyrosine. *MED1* is involved in the regulated transcription of nearly all RNA polymerase II-dependent genes. This gene does not show any single-phenotype association, but cross-phenotype analysis produced evidence of association. Using backward elimination, we find that phenylalanine and tyrosine are the last two phenotypes to be eliminated (Supporting Information Table S2). We have provided a detailed description of the function and clinical implications of the significant and suggestive genes in Supporting Information Table S4.

TABLE 3 *P* values for Multi-SKAT tests (Hom, Het, PhC, PC-Sel, and minP) with SKAT and Burden kernels for the genes reported in Table 2

Σ_G	Gene				Multi-SKAT					
	Name	Chromosome	Rare SNPs	MAC	minPhen	Hom	Het	PhC	PC-Sel	minP
	GLDC	9	4	183	6.8×10^{-63}	1.3×10^{-03}	1.3×10^{-17}	2.9×10^{-73}	5.3×10^{-59}	1.1×10^{-72}
	DHODH	16	5	90	5.1×10^{-08}	1.4×10^{-01}	3.2×10^{-03}	3.1×10^{-08}	7.1×10^{-06}	9.7×10^{-08}
	PAH	12	6	27	4.3×10^{-05}	7.9×10^{-02}	1.8×10^{-05}	3.9×10^{-07}	6.3×10^{-04}	1.4×10^{-06}
SKAT	*MED1*	17	3	147	8.7×10^{-02}	3.4×10^{-01}	9.3×10^{-07}	2.8×10^{-04}	1.9×10^{-04}	3.9×10^{-06}
	HAL	12	6	42	3.8×10^{-05}	5.5×10^{-01}	3.5×10^{-03}	2.9×10^{-06}	1.5×10^{-04}	1.1×10^{-05}
	STK33	11	6	180	4.0×10^{-01}	2.3×10^{-01}	8.9×10^{-06}	1.1×10^{-03}	5.7×10^{-03}	3.2×10^{-05}
	ALDH1L1	3	8	103	4.4×10^{-02}	1.1×10^{-01}	2.2×10^{-02}	1.6×10^{-04}	4.2×10^{-04}	3.8×10^{-04}
	BCAT2	19	3	133	9.7×10^{-04}	5.0×10^{-01}	8.1×10^{-02}	2.4×10^{-03}	3.5×10^{-03}	9.3×10^{-03}
	GLDC	9	4	183	1.4×10^{-59}	7.5×10^{-04}	1.5×10^{-15}	1.3×10^{-64}	2.1×10^{-54}	9.7×10^{-64}
	HAL	12	6	42	2.4×10^{-08}	2.8×10^{-05}	4.6×10^{-01}	4.2×10^{-12}	7.9×10^{-03}	4.2×10^{-11}
	PAH	12	6	27	4.3×10^{-05}	2.0×10^{-01}	5.3×10^{-04}	7.2×10^{-06}	9.3×10^{-03}	1.3×10^{-06}
Burden	*DHODH*	16	5	90	1.3×10^{-07}	5.3×10^{-02}	1.3×10^{-02}	2.9×10^{-06}	7.6×10^{-04}	7.7×10^{-06}
	BCAT2	19	3	133	8.4×10^{-06}	4.0×10^{-01}	1.7×10^{-02}	1.1×10^{-05}	6.1×10^{-03}	3.7×10^{-05}
	ALDH1L1	3	8	103	8.3×10^{-08}	1.7×10^{-02}	5.1×10^{-03}	2.1×10^{-06}	1.7×10^{-05}	4.2×10^{-05}
	MED1	17	3	147	9.4×10^{-01}	1.8×10^{-01}	8.7×10^{-05}	2.1×10^{-03}	7.1×10^{-01}	3.4×10^{-04}
	STK33	11	6	180	4.8×10^{-01}	7.1×10^{-01}	7.0×10^{-04}	3.8×10^{-02}	6.4×10^{-01}	6.3×10^{-03}

Note. Het: heterogeneous; Hom: homogeneous; MAF: minor allele frequency; minP: minimum *P* value; PC: principal component; PhC: phenotype covariance; SNP: single-nucleotide polymorphism; MAC: minor allele count.
Multi-SKAT tests were applied with the kinship adjustment, and 5,207 genes with at least three rare (MAF < 0.01) nonsynonymous and protein-truncating variants were used in this analysis. The total sample size was $n = 8,545$. *P* values smaller than the Bonferroni corrected significance $\alpha = 9.6 \times 10^{-6}$ were marked as bold. For the upper part of the table, minPhen was calculated as the Bonferroni-adjusted minimum SKAT *P* value across each phenotype, whereas for the lower part, it was calculated as the Bonferroni-adjusted minimum Burden *P* value across each phenotype.

TABLE 4 P values for genes reported in Table 2 using MSKAT, GAMuT, and Multi-SKAT (PhC and minP$_{com}$)

| Gene | Unrelated individuals ($n = 7{,}213$) | | | | | | All individuals ($n = 8{,}545$) | |
	MSKAT (Q)	MSKAT (Q')	GAMuT (Projection)	GAMuT (Linear)	PhC ($\Sigma_G = $ SKAT)	minPcom	PhC ($\Sigma_G = $ SKAT)	minPcom
GLDC	8.9×10^{-54}	6.1×10^{-15}	0^*	6.2×10^{-15}	8.1×10^{-54}	1.3×10^{-53}	2.9×10^{-73}	2.3×10^{-72}
HAL	9.5×10^{-05}	4.2×10^{-02}	9.6×10^{-05}	4.3×10^{-02}	9.5×10^{-05}	2.9×10^{-07}	2.9×10^{-06}	9.5×10^{-11}
DHODH	2.1×10^{-06}	2.2×10^{-03}	2.4×10^{-06}	2.2×10^{-03}	1.9×10^{-06}	8.3×10^{-06}	3.1×10^{-08}	1.1×10^{-07}
PAH	9.9×10^{-06}	1.3×10^{-02}	1.0×10^{-05}	1.3×10^{-02}	9.9×10^{-06}	5.1×10^{-05}	3.9×10^{-07}	1.9×10^{-06}
MED1	1.7×10^{-03}	2.7×10^{-01}	1.7×10^{-03}	2.7×10^{-01}	1.7×10^{-03}	2.8×10^{-05}	2.8×10^{-04}	4.9×10^{-06}
STK33	6.8×10^{-04}	6.9×10^{-01}	6.7×10^{-04}	6.9×10^{-01}	6.7×10^{-04}	1.9×10^{-06}	1.1×10^{-03}	4.2×10^{-05}
ALDH1L1	5.9×10^{-05}	3.1×10^{-02}	6.1×10^{-05}	3.0×10^{-02}	6.0×10^{-05}	9.5×10^{-06}	1.6×10^{-04}	5.4×10^{-05}
BCAT2	6.1×10^{-04}	1.5×10^{-02}	6.3×10^{-04}	1.5×10^{-02}	6.2×10^{-04}	3.7×10^{-05}	2.4×10^{-03}	6.2×10^{-05}

Note. minP: minimum P value; PhC: phenotype covariance.

P values in columns 2–7 were calculated with unrelated individuals ($n = 7{,}213$), whereas those in columns 8 and 9 were calculated using all individuals ($n = 8{,}545$). Both MSKAT (Q and Q' statistic) and GAMuT (projection and linear phenotype kernel) P values were calculated with the linear weighted genotype kernel. DKAT P values were nearly identical to those of GAMuT when the same kernels were used (data not shown). P values smaller than the Bonferroni corrected significance $\alpha = 9.6 \times 10^{-6}$ were marked as bold.

*GAMuT software collapses any P value lower than 10^{-50} to 0.

TABLE 5 Single-phenotype SKAT-O with kinship adjustment test for the METSIM study data ($n = 8{,}545$)

Gene	Ala	Gln	Gly	His	Ile	Leu	Phe	Tyr	Val
GLDC	2.9×10^{-01}	2.9×10^{-03}	2.5×10^{-64}	1.0×10^{-02}	1.5×10^{-01}	3.4×10^{-02}	8.5×10^{-01}	6.6×10^{-01}	4.7×10^{-03}
HAL	9.9×10^{-01}	1.1×10^{-01}	3.1×10^{-01}	3.2×10^{-09}	2.6×10^{-01}	2.5×10^{-01}	6.6×10^{-01}	1.2×10^{-01}	3.5×10^{-01}
DHODH	1.4×10^{-07}	9.9×10^{-01}	9.0×10^{-02}	3.6×10^{-01}	7.7×10^{-01}	1.7×10^{-01}	1.9×10^{-01}	3.0×10^{-01}	1.0×10^{-02}
PAH	7.9×10^{-01}	3.0×10^{-01}	2.8×10^{-01}	8.6×10^{-01}	4.5×10^{-01}	8.1×10^{-01}	6.8×10^{-05}	4.0×10^{-01}	9.9×10^{-01}
MED1	1.0×10^{-01}	5.1×10^{-01}	7.9×10^{-01}	5.9×10^{-01}	3.3×10^{-01}	1.4×10^{-01}	6.9×10^{-01}	6.8×10^{-02}	6.7×10^{-01}
STK33	8.4×10^{-01}	8.2×10^{-01}	3.5×10^{-01}	5.7×10^{-01}	6.6×10^{-01}	1.0×10^{-01}	9.9×10^{-01}	8.1×10^{-01}	4.1×10^{-01}
ALDH1L1	6.7×10^{-01}	7.6×10^{-01}	9.3×10^{-09}	7.3×10^{-01}	3.4×10^{-01}	3.2×10^{-01}	9.9×10^{-01}	5.9×10^{-01}	2.5×10^{-01}
BCAT2	1.4×10^{-01}	2.6×10^{-01}	8.2×10^{-01}	9.9×10^{-01}	1.0×10^{-01}	2.1×10^{-02}	5.4×10^{-01}	5.0×10^{-01}	1.2×10^{-06}

Note. Ala: alanine; Gln: glutamine; Gly: glycine; His: histidine; Ile: isoleucine; Leu: leucine; METSIM: METabolic Syndrome In Men; Phe: phenylalanine; Tyr: tyrosine; Val: valine.

P values smaller than the Bonferroni corrected significance $\alpha = 9.6 \times 10^{-6}$ were marked as bold.

Among other genes, *GLDC* has the smallest P value. Variants in *GLDC* are known to cause glycine encephalopathy (MIM: 605899; Hughes, 2009). To investigate whether our results were supported by single-phenotype associations, we applied SKAT-O to each of the nine amino acid phenotypes. Univariate SKAT-O test with each of these phenotype reveals that this gene has a strong association with glycine (P value $= 2.5 \times 10^{-64}$; Table 5). Among the variants genotyped in this gene, rs138640017 (MAF $= 0.009$) appears to drive the association (single-variant P value $= 1.0 \times 10^{-64}$). Variants in *HAL* cause histidinemia (MIM: 235800) in human and mouse. This gene shows significant univariate association with histidine (SKAT-O P value $= 3.2 \times 10^{-8}$; Table 5), which in turn is influenced by the association of rs141635447 (MAF $= 0.005$) with histidine (single-variant P value $= 3.7 \times 10^{-13}$). Similarly, variants in *DHODH*, which have been previously found to be associated with postaxial acrofacial dysostosis (MIM: 263750), have significant cross-phenotype association although the result is mostly driven by the association with alanine (SKAT-O P value $= 1.4 \times 10^{-07}$; Table 5). *ALDH1L1* catalyzes conversion of 10-formyltetrahydrofolate to tetrahydrofolate. Published results show that common variant rs1107366, 5 kb upstream of *ALDH1L1*, is associated with the glycine–creatinine ratio (Xie et al., 2013). Downregulation of *BCAT2* in mice causes elevated serum branched chain amino acid levels and features of maple syrup urine disease. Table 3 shows P values of Multi-SKAT kernel and minP with two genotype kernels

(SKAT and Burden). Among phenotype kernels, PhC and Het generally produced the smallest P values. We further applied Multi-SKAT tests without kinship adjustment on the whole METSIM study individuals. As expected, this produced inflation in QQ plots (Supporting Information Figure S5).

To directly compare our results with existing methods, we applied GAMuT, DKAT, and MSKAT to the METSIM data set. Because these methods cannot be applied to related individuals, we eliminated 1,332 individuals that were related up to second degree, leaving us 7,213 individuals. Table 4 shows P values of different methods on the eight significant or suggestive genes displayed in Table 2. Because DKAT and GAMuT had nearly identical P values when the same kernels were used, DKAT P values were not shown in Table 4. For unrelated individuals, as expected, P values produced by MSKAT with Q statistic, GAMuT with projection phenotype kernel and PhC (with SKAT Σ_G) were very similar, and minP$_{com}$ provided similar or more significant P values than PhC. Interestingly, MSKAT with Q' statistic and GAMuT with linear phenotype kernel have less significant P values than the other tests. We found that in five of the eight genes in Table 4, using all individuals with kinship correction produced more significant PhC and minP$_{com}$ P values than using only unrelated individuals. Further, we have listed the top 10 genes for each of PhC, GAMuT, and MSKAT with unrelated individuals (Supporting Information Table S4). Except for the genes in Table 4, no other genes were found to be significant or suggestive.

Overall, our METSIM amino acid data analysis suggests that the proposed method can be more powerful than the single-phenotype tests as well as existing tests, while maintaining Type I error rate even in the presence of the relatedness. It also shows that the omnibus tests (minP and minP$_{com}$) provide robust performance by effectively aggregating results of various kernels.

4.4 | Computation time

When Σ_P and Σ_G are given, P values of Multi-SKAT are computed by the Davies (1980) method, which inverts the characteristic function of the mixture of X^2. On average, Multi-SKAT tests for a given Σ_P and Σ_G required less than 1 CPU-sec (Intel Xeon 2.80 GHz, Produced by Intel Co., Santa Clara, CA) when applied to a data set with 5,000 independent individuals, 20 variants, and 10 phenotypes (Supporting Information Table S1). With the kinship adjustment for 5,000 related individuals, computation time was increased to 3 CPU-sec. Because minP$_{com}$ requires only a small number of resampling steps to

estimate the correlation among tests, it is still scalable for genome-wide analysis. In the same data set, minP$_{com}$ required 4 and 10 CPU-sec on average without and with the kinship adjustment, respectively. Further, Multi-SKAT, given Σ_P and Σ_G, is computationally equivalent to MSKAT and takes less than 1 CPU-sec for up to 20,000 samples, with 20 variants (Supporting Information Figure S7a), whereas GAMuT takes considerably more time than these two. The performance of minP$_{com}$ is similar to GAMuT for small and moderate sample sizes (7.5 and 7.1 CPU-sec, respectively, for 10,000 samples) and performs better than GAMuT for larger sample sizes (14.9 and 34.6 CPU-sec, respectively, for 20,000 samples). Computation times of all the methods were slightly increased when the number of variants was 100 (Supporting Information Figure S7b). Analyzing the METSIM data set with minP$_{com}$ required 10 hr when parallelized into five processes.

5 | DISCUSSION

In this study, we have introduced a general framework for rare-variant tests for multiple phenotypes. As demonstrated, Multi-SKAT gains flexibility with regard to modeling the relationship between phenotypes and genotypes through the use of the kernels Σ_P and Σ_G. Many published methods, including GAMuT, MSKAT, and MAAUSS, can be viewed as special cases of the Multi-SKAT test with corresponding values of Σ_P and Σ_G, which illuminates the underlying assumptions of these methods and their relationships. In addition, by unifying existing methods to the common framework, our approach provides a way to combine different methods through the minimum P value-based omnibus test. Our method can also adjust for sample relatedness. From simulation studies, we have found that the proposed method is scalable to genome-wide analysis and can outperform the single-phenotype test and existing multiple-phenotype tests. The METSIM data analysis demonstrated that the proposed methods perform well in practice.

It is natural to assume that different genes follow different models of association. For some genes, the effect of the variants on the phenotypes might be independent of each other, thus best detected by the Het phenotype kernel for Σ_P, whereas for others, the effects might be nearly the same and best detected by the Hom phenotype kernel. If the kernel structures are chosen based on prior knowledge and the selected Σ_G and Σ_P do not reflect underlying biology, the test may have substantially reduced power. The omnibus test, which uses the minimum P value from the various choices of kernels, has been a useful approach under such situations in

genetic association analysis (Lee, Wu et al., 2012; Urrutia et al., 2015; Zhan et al., 2017). We applied this omnibus test to Multi-SKAT and used a Copula to obtain P values. As seen in simulation studies and real data analysis, our omnibus approaches (minP and $minP_{com}$) are scalable to genome-wide analysis and provide robust power regardless of underlying genetic models.

Multi-SKAT retains most of the desirable properties of SKAT. The asymptotic P values of all the Multi-SKAT tests, other than minP and $minP_{com}$, can be analytically obtained via Davies' method. The P value calculations for minP and $minP_{com}$ depend on a resampling-based approach but a reliable estimate can be obtained using a small number of resampling steps. Thus, computationally, all the Multi-SKAT tests are scalable at the genome-wide level. This method also allows the inclusion of prior information through weighting of variants.

Additionally, Multi-SKAT can adjust for the relatedness among study individuals by accounting for their kinship matrix. As shown in Supporting Information Figure S5, in the presence of related individuals, lack of adjustment for relatedness can produce inflated Type I error rate. Because Multi-SKAT is a regression-based approach, it effectively incorporates the relatedness by including a random effect term for kinship. Type I error simulation and METSIM data analysis show that our approach produced more significant P values than alternative methods, like GAMuT and MSKAT, while controlling Type I error rates.

Although Multi-SKAT provides a general framework for gene-based multiple-phenotype tests, the current approach is limited to continuous phenotypes. In the future, using a generalized mixed effect model framework, we aim to extend Multi-SKAT to binary phenotypes.

In summary, we have developed a powerful multiple-phenotype test for rare variants. The proposed method has robust power regardless of the underlying biology and can adjust for family relatedness. Our method can be a scalable and practical solution to test for multiple phenotypes and will contribute to detecting rare variants with pleiotropic effects. All our methods are implemented in the R-package Multi-SKAT (see Web Resource).

6 | WEB RESOURCES

Multi-SKAT R-package: https://github.com/diptavo/MultiSKAT.
GAMuT R-package: https://epstein-software.github.io/GAMuT.
MSKAT R-package: https://github.com/baolinwu/MSKAT.

PHENIX R-package: https://mathgen.stats.ox.ac.uk/genetics/_software/phenix/phenix.html.
KING: http://people.virginia.edu/~wc9c/KING/
Online Mendelian Inheritance in Man (OMIM): http://www.omim.org.

ORCID

Diptavo Dutta http://orcid.org/0000-0002-6634-9040
Seunggeun Lee http://orcid.org/0000-0002-8097-3878

REFERENCES

Allan Butterfield, D., & Pocernich, C. B. (2003). The glutamatergic system and Alzheimer's disease. *CNS Drugs*, *17*(9), 641–652.

Aschard, H., Vilhjálmsson, B. J., Greliche, N., Morange, P.-E., Trégouët, D.-A., & Kraft, P. (2014). Maximizing the power of principal-component analysis of correlated phenotypes in genome-wide association studies. *The American Journal of Human Genetics*, *94*(5), 662–676.

Broadaway, K. A., Cutler, D. J., Duncan, R., Moore, J. L., Ware, E. B., Min, A., & Epstein, M. P. (2016). A statistical approach for testing cross-phenotype effects of rare variants. *The American Journal of Human Genetics*, *98*(3), 525–540.

Bulik-Sullivan, B. K., Loh, P.-R., Finucane, H. K., Ripke, S., Yang, J., of the Psychiatric Genomics Consortium, Neale, B. M. (2015). Ld score regression distinguishes confounding from polygenicity in genome-wide association studies. *Nature Genetics*, *47*, 291–295.

Chiu, C., Jung, J., Wang, Y., Weeks, D., Wilson, A., Bailey-Wilson, J., & Fan, R. (2017). A comparison study of multivariate fixed models and gene association with multiple traits (gamut) for next generation sequencing. *Genetic Epidemiology*, *41*(1), 18–34.

Cotsapas, C., Voight, B. F., Rossin, E., Lage, K., Neale, B. M., Wallace, C. ... Daly, M. J. (2011). Pervasive sharing of genetic effects in autoimmune disease. *PLOS Genetics*, *7*(8), e1002254.

Dahl, A., Iotchkova, V., Baud, A., Johansson, A., Gyllensten, U., Soranzo, N., & Marchini, J. (2016). A multiple-phenotype imputation method for genetic studies. *Nature Genetics*, *48*, 466–472.

Davies, R. B. (1980). The distribution of a linear combination of X^2 random variables. *Applied Statistics*, *29*(3), 323–333.

de Belleroche, J., Recordati, A., & Clifford, F. (2003). Elevated levels of amino acids in the CSF of motor neuron disease patients. *CNS Drugs*, *17*(9), 641–652.

Demarta, S., & McNeil, A. J. (2005). The t Copula and related Copulas. *International Statistical Review/Revue Internationale de Statistique*, *73*(1), 111–129.

Ferreira, M., & Purcell, S. (2009). A multivariate test of association. *Bioinformatics*, 25, 132–133.

He, Z., Xu, B., Lee, S., & Ionita-Laza, I. (2017). Unified sequence-based association tests allowing for multiple functional annotations and meta-analysis of noncoding variation in metabochip data. *The American Journal of Human Genetics*, 101(3), 340–352.

Huang, J., Johnson, A., & O'Donnell, C. (2011). Prime: A method for characterization and evaluation of pleiotropic regions from multiple genome-wide association studies. *Bioinformatics*, 27(9), 1201–1206.

Hughes, I. (2009). Pediatric endocrinology and inborn errors of metabolism. *Journal of Paediatrics and Child Health*, 45(11), 668–669.

Huyghe, J. R., Jackson, A. U., Fogarty, M. P., Buchkivoch, M. L., Stancakova, A., Stringham, H. M. ... Mohlke, K. L. (2013). Exome array analysis identifies new loci and low-frequency variants influencing insulin processing and secretion. *Nature Genetics*, 45, 197–201.

Ionita-Laza, I., Capanu, M., De Rubeis, S., McCallum, K., & Buxbaum, J. D. (2014). Identification of rare causal variants in sequence-based studies: Methods and applications to vps13b, a gene involved in Cohen syndrome and autism. *PLOS Genetics*, 10(12), e1004729.

Korte, A., & Farlow, A. (2013). The advantages and limitations of trait analysis with GWAS: A review. *Plant Methods*, 9, 9–29.

Lee, S., Abecasis, G. R., Boehnke, M., & Lin, X. (2014). Rare-variant association analysis: Study designs and statistical tests. *The American Journal of Human Genetics*, 95(1), 5–23.

Lee, S., Emond, M. J., Bamshad, M. J., Barnes, K. C., Rieder, M. J., Nickerson, D. A. ... Lin, X. (2012). Optimal unified approach for rare-variant association testing with application to small-sample case-control whole-exome sequencing studies. *The American Journal of Human Genetics*, 91(2), 224–237.

Lee, S., Won, S., Kim, Y. J., Kim, Y., Kim, B.-J., & Park, T. (2016). Rare variant association test with multiple phenotypes. *Genetic Epidemiology*, 41, 198–209.

Lee, S., Wu, M. C., & Lin, X. (2012). Optimal tests for rare variant effects in sequencing association studies. *Biostatistics*, 13(4), 762–775.

Maity, A., Sullivan, P., & Tzeng, J. (2012). Multivariate phenotype association analysis by marker-set kernel machine regression. *Genetic Epidemiology*, 36, 686–695.

Manichaikul, A., Mychaleckyj, J. C., Rich, S. S., Daly, K., Sale, M., & Chen, W. M. (2010). Robust relationship inference in genome-wide association studies. *Bioinformatics*, 26(22), 2867–2873.

Ray, D., Pankow, J. S., & Basu, S. (2016). USAT: A unified score-based association test for multiple phenotype-genotype analysis. *Genetic Epidemiology*, 40(1), 20–34.

Ried, J. S., Doring, A., Oexle, K., Meisinger, C., Winkelmann, J., Klopp, N., & Gieger, C. (2012). PSEA: Phenotype set enrichment analysis—A new method for analysis of multiple phenotypes. *Genetic Epidemiology*, 36, 244–252.

Schaffner, S. F., Foo, C., Gabriel, S., Reich, D., Daly, M. J., & Altshuler, D. (2005). Calibrating a coalescent simulation of human genome sequence variation. *Genome Research*, 15(11), 1576–1583.

Sivakumaran, S., Agakov, F., Theodoratou, E., Prendergast, J. G., Zgaga, L., Manolio, T., & Campbell, H. (2011). Abundant pleiotropy in human complex diseases and traits. *The American Journal of Human Genetics*, 89(5), 607–618.

Solovieff, N., Cotsapas, C., Lee, P. H., Purcell, S. M., & Smoller, J. W. (2013). Pleiotropy in complex traits: Challenges and strategies. *Nature Reviews. Genetics*, 14(7), 483.

Stančáková, A., Civelek, M., Saleem, N., Soininen, P., Kangas, A., Cederberg, H. ... Laakso, M. (2012). Hyperglycemia and a common variant of GCKR are associated with the levels of eight amino acids in 9,369 Finnish men. *Diabetes*, 61, 1895–1902.

Sun, J., Oualkacha, K., Forgetta, V., Zheng, H.-F., Richards, J. B., Ciampi, A., & Greenwood, C. M. (2016). A method for analyzing multiple continuous phenotypes in rare variant association studies allowing for flexible correlations in variant effects. *European Journal of Human Genetics*, 24(9), 1344–1351.

Tajiri, K., & Shimizu, Y. (2013). Branched-chain amino acids in liver diseases. *World Journal of Gastroentology*, 19, 7620–7629.

Teslovich, T. M., Kim, D. S., Yin, X., Stancakova, A., Jackson, A. U., Weilscher, M. ... Mohlke, K. L. (2018). Identification of seven novel loci associated with amino acid levels using single-variant and gene-based tests in 8545 Finnish men from the METSIM study. *Human Molecular Genetics*, 27, 1664–1674.

Urrutia, E., Lee, S., Maity, A., Zhao, N., Shen, J., Li, Y., & Wu, M. (2015). Rare variant testing across methods and thresholds using the multi-kernel sequence kernel association test (MK-SKAT). *Statistics and Its Interface*, 8(4), 495–505.

Wang, Y., Liu, A., Mills, J., Boehnke, M., Wilson, A., Bailey-Wilson, J., & Fan, R. (2015). Pleiotropy analysis of quantitative traits at gene level by multivariate functional linear models. *Genetic Epidemiology*, 39, 259–275.

Würtz, P., Mäkinen, V.-P., Soininen, P., Kangas, A., Tukiainen, T., Kettunen, J. ... Ala-Korpela, M. (2012). Metabolic signatures of insulin resistance in 7,098 young adults. *Diabetes*, 61, 1372–1380.

Würtz, P., Soininen, P., Kangas, A., Rönnemaa, T., Lehtimäki, T., Kähönen, M., & Ala-Korpela, M. (2013). Branched-chain and aromatic amino acids are predictors of insulin resistance in young adults. *Diabetes Care*, 36, 648–655.

Wu, B., & Pankow, J. (2016). Sequence kernel association test of multiple continuous phenotypes. *Genetic Epidemiology*, 40(2), 91–100.

Wu, M. C., Lee, S., Cai, T., Li, Y., Boehnke, M., & Lin, X. (2011). Rare-variant association testing for sequencing data with the sequence kernel association test. *American Journal of Human Genetics*, 89, 82–93.

Wu, M. C., Maity, A., Lee, S., Simmons, E. M., Harmon, Q.E., Lin, X., ... Armistead, P. M. (2013). Kernel machine SNP-set testing under multiple candidate kernels. *Genetic Epidemiology*, 37(3), 267–275.

Xie, W., Wood, A. R., Lyssenko, V., Weedon, M. N., Knowles, J. W., Alkayyali, S. ... Walker, M. (2013). Genetic variants associated with glycine metabolism and their role in insulin sensitivity and type 2 diabetes. *Diabetes*, 62, 2141–2150.

Yan, Q., Weeks, D. E., Celedón, J. C., Tiwari, H. K., Li, B., Wang, X. ... Liu, N. (2015). Associating multivariate quantitative phenotypes with genetic variants in family samples with a novel kernel machine regression method. *Genetics*, 201(4), 1329–1339.

Zhan, X., Zhao, N., Plantinga, A., Thornton, T., Conneely, K., Epstein, M., & Wu, M. (2017). Powerful genetic association analysis for common or rare variants with high-dimensional structured traits. *Genetics*, 206(4), 1779–1790.

Zhou, X., Carbonetto, P., & Matthew, S. (2013). Polygenic modeling with Bayesian sparse linear mixed models. *PLOS Genetics*, 9(2), e1003264.

Zhou, X., & Stephens, M. (2014). Efficient multivariate linear mixed model algorithms for genome-wide association studies. *Nature Methods*, 11(4), 407–409.

SUPPORTING INFORMATION

Additional supporting information may be found online in the Supporting Information section at the end of the article.

APPENDIX A: PRINCIPAL COMPONENT (PC) KERNEL

Let L_i be the loading vector for the ith PC, which produces the ith PC score $P_i = YL_i$. In PCA-based analysis, PC scores are used as outcomes instead of original Y. Because the genetic information regarding the phenotypes may not be confined to the top few PCs (Aschard et al., 2014), we first consider using all PCs. Let $P = (P_1, ..., P_K)$. Because PCs are orthogonal, we assume genetic effects to multiple PCs are heterogeneous, which resulted in

$$Q = \{\text{vec}(P) - \text{vec}(\hat{\mu}_P)\}^T \{(G\Sigma_G G^T) \otimes (\widehat{V}_P^{-1} \widehat{V}_P^{-1})\}\{\text{vec}(P) - \text{vec}(\hat{\mu}_P)\}, \tag{A1}$$

where $\hat{\mu}_P$ is the mean of P under the null hypothesis and $\widehat{V}_P$ the estimated covariance matrix between the PCs. $\widehat{V}_P$ will be a diagonal matrix because PCs are orthogonal. Equation (A1) can be written as

$$Q = \{\text{vec}(Y) - \text{vec}(\hat{\mu})\}^T \{(G\Sigma_G G^T) \otimes (L\widehat{V}_P^{-1} \widehat{V}_P^{-1} L^T)\}\{\text{vec}(Y) - \text{vec}(\hat{\mu})\}, \tag{A2}$$

where $L = (L_1, ..., L_K)$ is a $K \times K$ PC loading matrix. Equation (A2) shows that by using $\Sigma_{P,\text{PC}} = \widehat{V}L\widehat{V}_P^{-1}\widehat{V}_P^{-1}L^T\widehat{V}$, we can carry out PC-based tests. It is to

be noted that the genetic effects of the PCs do not need to be assumed to be heterogeneous. Any kernel structure that is applicable to the test statistic in Equation (4) can be applied here as well.

APPENDIX B: RELATIONSHIP BETWEEN MULTI-SKAT AND EXISTING METHODS

For the ease of algebraic expressions, we will consider that all the K phenotypes have residual variance 1. For the general case of different residual variances, Σ_P should be replaced by $T_w^{-1}\Sigma_P T_w^{-1}$, where $T_w = \text{diag}(\sigma_1, ..., \sigma_K)$, σ_k being the residual standard error of kth phenotype.

B.1 | MSKAT

The Q statistic of MSKAT (Wu & Pankow, 2016) is given by

$$Q_{\text{MSKAT}} = \text{vec}(S_c)^T (WW \otimes \widehat{V}^{-1})\text{vec}(S_c), \tag{B1}$$

where $S_c = G^T(Y - \hat{\mu})$ is a matrix of score statistics (Wu & Pankow, 2016). Using row-vectorization properties,

$$\text{vec}(S_c) = \text{vec}(G^T(Y - \hat{\mu})) = (G^T \otimes I)\text{vec}(Y - \hat{\mu})$$
$$= (G^T \otimes I)\{\text{vec}(Y) - \text{vec}(\hat{\mu})\}.$$

Then Q_{MSKAT} can be written as

$$\{\text{vec}(Y) - \text{vec}(\hat{\mu})\}^T \{(GWWG^T) \otimes \widehat{V}^{-1}\}\{\text{vec}(Y) - \text{vec}(\hat{\mu})\},$$

which is the Multi-SKAT test statistics with $\Sigma_G = WW$ and $\Sigma_P = \widehat{V}$.

Further, the Q' of MSKAT is given by

$$Q'_{\text{MSKAT}} = \text{vec}(S_c)^T (WW \otimes I)\text{vec}(S_c). \tag{B2}$$

Using the similar algebra as above, this can be written as

$$\{\text{vec}(Y) - \text{vec}(\hat{\mu})\}^T \{(GWWG^T) \otimes I\}\{\text{vec}(Y) - \text{vec}(\hat{\mu})\},$$

which is the Multi-SKAT test statistics with $\Sigma_G = WW$ and $\Sigma_P = \widehat{V}^2$.

B.2 | GAMuT

Suppose $Y - \widehat{\mu} = Y_{\text{adj}} = HY$ and $G_{\text{adj}} = HG$ are covariate-adjusted phenotype and genotype matrices, where $H = I - X(X^T X)^{-1} X^T$. With the intercept in X, Y_{adj} and G_{adj} are mean centered. The covariate-adjusted GAMuT test statistics is

$$Q_{\text{GAMuT}} = \frac{\text{tr}(P_c X_c)}{n},$$

where

$$P_c = \begin{cases} Y_{\text{adj}}(Y_{\text{adj}}^T Y_{\text{adj}})^{-1} Y_{\text{adj}}^T & \text{for projection phenotype} \\ & \text{kernel,} \\ Y_{\text{adj}} Y_{\text{adj}}^T & \text{for linear phenotype kernel} \end{cases}$$

and $X_c = G_{\text{adj}} WW G_{\text{adj}}^T$. Using the fact that $Y_{\text{adj}}^T Y_{\text{adj}}/n = \widehat{V}$ is the estimate of variance after adjusting covariates and $G_{\text{adj}}^T Y_{\text{adj}} = G^T HY = G^T Y_{\text{adj}}$ (because H is a symmetric idempotent matrix), we show, for the projection kernel,

$$\begin{aligned} \text{tr}(P_c X_c)/n &= \text{tr}(Y_{\text{adj}} \widehat{V}^{-1} Y_{\text{adj}}^T G_{\text{adj}} WW G_{\text{adj}}^T) \\ &= \text{tr}(\widehat{V}^{-\frac{1}{2}} Y_{\text{adj}}^T GWW G^T Y_{\text{adj}} \widehat{V}^{-\frac{1}{2}}) \\ &= \text{vec}(WG^T Y_{\text{adj}} \widehat{V}^{-\frac{1}{2}})^T \text{vec}(WG^T Y_{\text{adj}} \widehat{V}^{-\frac{1}{2}}) \\ &= \{(WG^T \otimes \widehat{V}^{-\frac{1}{2}})\text{vec}(Y_{\text{adj}})\}^T \{(WG^T \otimes \widehat{V}^{-\frac{1}{2}}) \\ & \quad \text{vec}(Y_{\text{adj}})\} \\ &= \{\text{vec}(Y) - \text{vec}(\widehat{\mu})\}^T (GWW G^T \otimes \widehat{V}^{-1}) \\ & \quad \{\text{vec}(Y) - \text{vec}(\widehat{\mu})\}, \end{aligned}$$

which is the same as the Multi-SKAT test statistic with $\Sigma_G = WW$ and $\Sigma_P = \widehat{V}$. Similarly for the linear kernel,

$$\begin{aligned} \text{tr}(P_c X_c)/n &= \text{tr}(Y_{\text{adj}} Y_{\text{adj}}^T G_{\text{adj}} WW G_{\text{adj}}^T) \\ &= \{(WG^T \otimes I)\text{vec}(Y_{\text{adj}})\}^T \{(WG^T \otimes I) \\ & \quad \text{vec}(Y_{\text{adj}})\} \\ &= \{\text{vec}(Y) - \text{vec}(\widehat{\mu})\}^T (GWW G^T \otimes I) \\ & \quad \{\text{vec}(Y) - \text{vec}(\widehat{\mu})\}, \end{aligned}$$

which is the Multi-SKAT test statistic with $\Sigma_G = WW$ and $\Sigma_P = \widehat{V}^2$.

B.3 | MAAUSS and MF-KM

There exist two different versions of the MAAUSS tests. The homogeneous version of MAAUSS assumes that the effects of a variant on multiple phenotypes are identical and use the following test statistic:

$$\begin{aligned} Q_{\text{MAAUSS-HOM}} &= (\text{vec}(Y) - \text{vec}(\widehat{\mu}))^T (I_n \otimes \widehat{V}^{-1}) \\ & \quad (G \otimes I)(WW \otimes 1_m 1_m^T)(G^T \otimes I) \\ & \quad (I_n \otimes \widehat{V}^{-1})(\text{vec}(Y) - \text{vec}(\widehat{\mu})), \quad \text{(B3)} \end{aligned}$$

which is identical to the Multi-SKAT test statistic with $\Sigma_G = WW$ and $\Sigma_P = 1_m 1_m^T$. The heterogeneous version of MAAUSS assumes that the effects of a variant on multiple phenotypes are independent and use the following test statistic:

$$\begin{aligned} Q_{\text{MAAUSS-HET}} &= (\text{vec}(Y) - \text{vec}(\widehat{\mu}))^T (I_n \otimes \widehat{V}^{-1}) \\ & \quad (G \otimes I)(WW \otimes I)(G^T \otimes I) \\ & \quad (I_n \otimes \widehat{V}^{-1})(\text{vec}(Y) - \text{vec}(\widehat{\mu})), \quad \text{(B4)} \end{aligned}$$

which is identical to the Multi-SKAT test statistic with $\Sigma_G = WW$ and $\Sigma_P = I$. Note that the test statistic of MF-KM is exactly the same as $Q_{\text{MAAUSS-HET}}$.

APPENDIX C: BACKWARD ELIMINATION PROCEDURE TO IDENTIFY ASSOCIATED PHENOTYPES

After identifying the gene or region associated with multiple phenotypes, next question would be identifying truly associated phenotypes. Here, we present a simple backward elimination algorithm to iteratively remove relatively less important phenotypes. A similar method has previously been applied to identify rare causal variants in an associated gene (Ionita-Laza et al., 2014).

- *Step* 1. Start with a set of k phenotypes $\text{Phen}_{\text{Current}} = \{y_1, y_2, ..., y_k\}$ and compute a Multi-SKAT test association P value for the set $\text{Phen}_{\text{Current}}$ denoted by p_{Current}.
- *Step* 2. Remove each of the phenotypes one at a time from the set $\text{Phen}_{\text{Current}}$. The resulting set is $\text{Phen}_{-i} = \{y_1, y_2, ..., y_{i-1}, y_{i+1}, ..., y_k\}$ for $i = 1, 2, ..., k$ and computes the corresponding P values p_{-i} for that the same Multi-SKAT test.

- *Step* 3. Remove the phenotype j that leads to the smallest P value, that is, $j = \mathrm{argmin}\{p_{-1}, p_{-2}, ..., p_{-k}\}$. Update $\mathrm{Phen}_{\mathrm{Current}}$ to Phen_{-j}.
- *Step* 4. Continue removing phenotypes till only one phenotype is left.

Supporting Information Table S2 shows the backward elimination results of five most significant and suggestive genes in the METSIM study data analysis as per the P values reported by $\mathrm{minP}_{\mathrm{com}}$. Although this procedure does not provide a set of phenotypes truly associated, it provides the relative importance of the phenotypes in driving association signals. For example, the $\mathrm{minP}_{\mathrm{com}}$ P value for *GLDC* was 2.3×10^{-72}. When each of the phenotypes was removed one at a time and the $\mathrm{minP}_{\mathrm{com}}$ P values were calculated on the remaining eight phenotypes, we found that eliminating isoleucine (Ile) actually improved the signal. The $\mathrm{minP}_{\mathrm{com}}$ P value of the set of eight amino acids leaving out Ile was 2.8×10^{-73}. This indicates that isoleucine has very minimal contribution to the association between the amino acids and *GLDC*. Subsequently, valine was the next phenotype to be eliminated indicating that it has the next lowest contribution after isoleucine. Carrying out this procedure further, we find that glycine is the last phenotype to remain indicating that it is the strongest driver of the signal. This is in agreement to the single-phenotype SKAT-O results (Table 5). Similarly for genes *HAL*, *DHODH*, *PAH*, and *MED1*, histidine, alanine, phenylalanine, and tyrosine were the most associated phenotypes, respectively. Interestingly for *PAH* and *MED1*, single-phenotype P values are not significant, which suggests that multiple phenotypes are associated with these genes.